

Fracture Behavior of Metal Foam Made of Recycled MMC by the Melt Route

Emiel Amsterdam¹, Norbert Babcsán², Jeff T.M. De Hosson¹, Patrick R. Onck¹, John Banhart²

¹ Department of Applied Physics, the Netherlands Institute for Metals research and Materials Science Center, University of Groningen, Nijenborgh 4, 9747 AG Groningen, the Netherlands

² Hahn-Meitner-Institut Berlin, Glienicke Str. 100, D-14109 Berlin and Technical University Berlin, Institute of Materials Science and Technology, Hardenbergstr. 36, D-10632 Berlin, Germany

Metal foam was made from recycled MMC precursor by the melt route. The original starting material was an Al-9Si alloy containing 20 vol% of SiC particles (10 μm), which are used to stabilize the foam during the foaming process. The starting material has been used to make foam parts from which the residue was recycled and refoamed. During the (re)foaming process Fe is present in the melt. During solidification of the foam, $\beta\text{-AlSiFe}$ plates are formed with the surplus of Si and Al present in the alloy. These plates run through the entire thickness of the cell wall (40-50 μm) and their length ranges between 50 and 200 μm . During *in-situ* tensile tests fracture initiates in the $\beta\text{-AlFeSi}$ plates and propagates through other $\beta\text{-AlFeSi}$ plates leading to brittle fracture of the cell walls.

Keywords: metal foam, processing, precipitation, AlFeSi, mechanical properties, fracture, microstructure

1. Introduction

The quality of aluminum foam made by the melt route has increased considerably over the last few years^{1,2}. The number of imperfections, such as missing and buckled cell walls, have decreased resulting in stiffer and stronger foams (see fig. 1). However, next to the cellular structure also the microstructure of the aluminum has a high influence on the fracture behavior of the aluminum foam, as shown in references 3 and 4. The objective of this study is to look at the fracture behavior of metal foam, made from recycled MMC by the melt route. We study crack initiation and propagation in cell walls under tensile stress and relate this to the microstructure of the foam. This information will contribute to improved manufacturing procedures to make tougher foams with an enhanced ability of recycling of the MMC melt. The paper is organized as follows. In the following section the material is described and the experimental procedures are explained. In the subsequent section the experimental observations are reported; first the microstructure is thoroughly investigated and described, followed by the results on the fracture behavior from the tensile tests.

2. Material and Experimental Procedures

2.1 Material and foaming procedure

The material of investigation is Duralcan metal matrix composite (MMC). The MMC has a cast Al-9Si aluminum alloy matrix reinforced by 20 vol% SiC particles with a mean particle size of 10 μm . The original composition of the raw materials is listed in Table 1. The MMC first was processed into foam parts, then these foams were remelted and this melt was refoamed. The foam was produced in both cases by gas injection into a melt in an adiabatic furnace. Air was used as foaming gas. Due to a special foam generator the bubble formation was well controlled. The gas bubbles could float towards the melt surface where liquid-aluminum foam is generated. The foaming temperature was kept around 700°C (above liquidus). The

thickness of the cell wall is about 40-50 μm and the diameters of the pores are about 5-7 mm. The density is 0.11 g/cm^3 , meaning a relative density of 4.0 % compared to pure aluminum (2.7 g/cm^3).

2.2 Experimental equipment and procedures

A Philips/FEI XL30-FEG environmental scanning electron microscope (ESEM) was used for the characterization of the microstructure of the aluminum foam as well as for the *in-situ* tensile tests. To investigate grain orientations using Orientation Imaging Microscopy (OIM) an electron backscatter detector is attached to an XL30S FEG-SEM, both SEMs are equipped with detectors for energy-dispersive X-ray spectroscopy (EDS). A tensile stage made by Kamrath&Weiss was used for the *in-situ* SEM tensile tests. During the *in-situ* tensile tests the image of the SEM was recorded on video to see the exact point of crack initiation and secondary electron (SE) images as well as backscatter-electron (BSE) images of the cell walls are taken before and after the tensile test. The displacement rate for *in-situ* tensile tests is 300 $\mu\text{m}/\text{min}$ and the maximum dimensions of the foam test

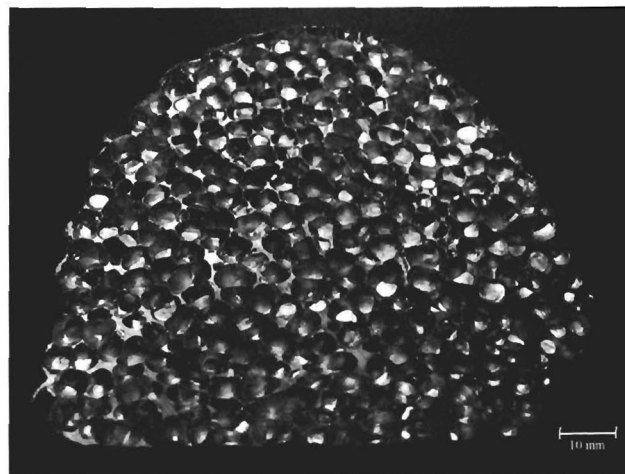


Fig. 1 Macrostructure of the metal foam made by the melt route

Table 1 Chemical composition (wt%) of the precursor (stated by the supplier) and of the foam measured by an EDS scan of the area in figure 2a. EDS-1 is calculated by only taking the peaks of the alloying elements into account, while EDS-2 takes all peaks of the spectrum into account.

Element	Si	Fe	Mg	Cu	Ti	C	O	SiC	Al
precursor	9	0.16	0.6	0.2 max	0.12			20 vol %	Bal.
EDS-1	15.61	0.69	0.55						83.15
EDS-2	14.63	0.66	0.53			1.61	2.44		80.12

samples are 4x10x15 mm (excluding clamping blocks). With this size the thickness of the samples (4 mm) is less than the cell size of the foam and therefore these samples had only one cell wall in the thickness, which makes them suitable for observing the fracture behavior in a cell wall, but not for quantitative tensile tests. For a quantitative tensile stress-strain measurement an ex-situ tensile test was performed in a displacement control manner on a MTS 810 servo-hydraulic test machine with a load cell of 10 kN. The foam sample had the following dimensions, 50x50x50 mm, so as to ensure at least 7 cells in each direction. In both cases, in-situ and ex-situ, the foam samples were glued on both sides to steel blocks with an epoxy-glue (Araldite 2011) made by Vantico. The aluminum blocks with the foam glued in between could easily be clamped inside the tensile stages without deforming the foam prior to the tensile test.

3. Results

3.1 Microstructural characterizations

The microstructure of the foam consists of dendrites of a-Al and eutectic structure of Al and Si (see fig. 2). SiC particles are located just below the gas/aluminum interface and between the particles there is a high amount of Si. The chemical composition was examined with energy-dispersive X-ray spectroscopy (EDS) on the entire area of figure 2a and the result is listed in table 1. The concentration of Si and Fe is higher than that of the precursor. The distribution of Fe, which was measured with EDS, can be made visible with EDS color mapping and it shows that the Fe is concentrated in the white needles seen in figure 2a. The composition of these needles has been measured and they are likely to be plates of β -AlFeSi. β -AlFeSi (Al_5FeSi) phase has a monoclinic crystal structure and a plate-like morphology, which look like needles in an embedded and polished cross-section. EDS spectra taken from the β -phase showed a Fe/Si (at.%) ratio of approximately 1 in the chemical composition⁵. The β -AlFeSi has a sharp interface boundary and the highly faceted nature may induce significant stresses in the aluminum matrix acting as a potential site for crack initiation. The β -phase is dominant at high silicon content and low cooling rates. The size of the AlFeSi-precipitates increases with decreasing cooling rates and scales with the amount of Fe in the aluminum alloy⁶⁻⁸. The size of these needles appears to be about 50-200 μm and they are randomly oriented and homogeneously distributed. The amount of Fe is about 4 times higher than the amount of Fe in the precursor (see table 1). In order to confirm the EDS measurements, the amount of needles were calculated with the assumption that all the Fe forms Al_5SiFe upon solidification. This assumption is valid

because the solubility of Fe in Al is negligibly small and there is an abundance of Al and Si⁹. The calculated amount of needles is 2.21% of the area (density and average atomic weight were taken into account). The amount of area covered by the needles can also be calculated by image analysis. The contrast and brightness of the image of the scanned area (fig. 2a) was adjusted so that the Al appears black and all the needles appear grey/white. Using a Matlab code the percentage of grey pixels was plotted against the threshold. The amount of needles estimated by image analysis is 2.5% +/- 0.5% (the error originates from the inaccuracy in choosing the threshold). This result matches quite nicely to the results obtained from EDS measurement of the needles. The needles were observed in the same quantity throughout the large foam sample, tacitly assuming that all the Fe goes into Al_5SiFe , so that the amount of Fe is distributed uniformly throughout the foam sample. The grain size is about 500-1000 μm which is much larger than the dendritic structure and the β -AlFeSi plates. There seems to be no difference between the grain size in the struts and the cell walls. Some β -AlFeSi plates run from one grain into another.

3.2 Fracture analysis

Figure 3 shows the stress-strain curve for the ex-situ tensile stress-strain test of the large foam sample

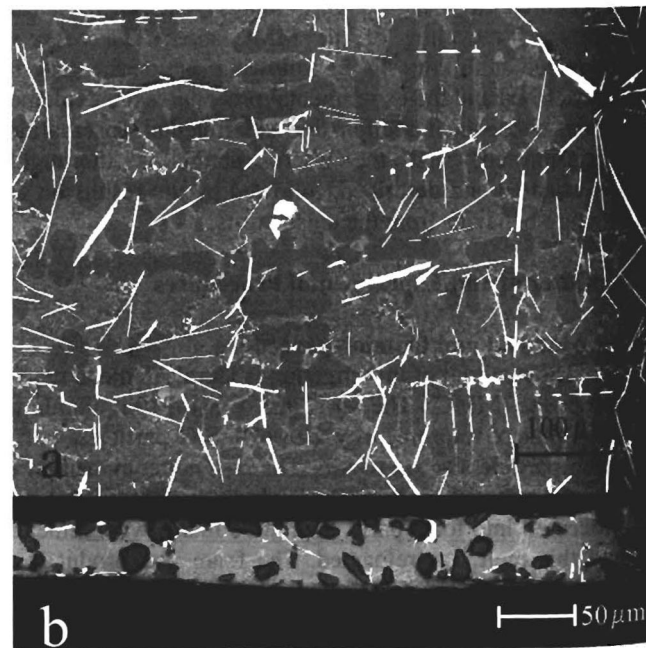


Fig. 2: (a) BSE image of an embedded and polished cross-section of a strut showing the microstructure. Dendrites of a-Al and eutectic structure of Al-Si with needles of β -AlFeSi (white) (b) Embedded and polished cross-section of a cell wall. The dark inclusions are the SiC particles.

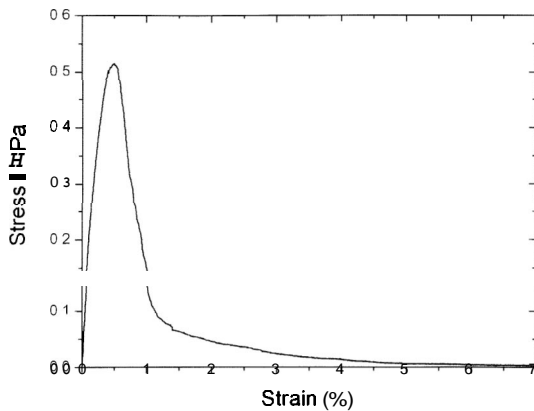


Fig. 3: Tensile stress-strain curve of the large foam sample (50x50x50 mm) with 4.0% relative density.

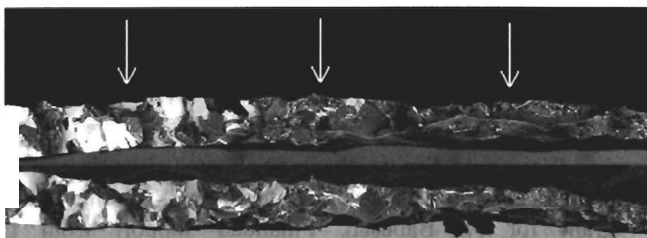


Fig. 4: Fracture surfaces of a cell wall width. Left arrow indicates cleavage of a β -AlFeSi plate. Middle arrow indicates fractured SiC particles and dimples with Si and the right arrow indicates ductile Al fracture. Upper fracture surface is mirrored for convenience.

(50x50x50 mm) of 4.0 % relative density. The curve displays a very long linear behavior until 0.5 MPa and at 0.51 MPa the ultimate tensile strength (UTS) is reached at a strain to failure of only 0.5 %. After the peak the stress drops rapidly, due to fast crack propagation and the curve ends with a long tail common to metal foams. The fracture surfaces of the cell walls exhibit three types of features (see fig. 4); the first is the cleavage of the SiC particles surrounded by dimples caused by the high amount of Si between the SiC. Other areas show cleavage of the β -AlFeSi plates, which run through the thickness of the entire cell wall having a length of about 200 μm (see fig. 4 and 6c). Only a small amount of area fractured in a ductile manner via necking of the u-Al. This is probably due to the fact that the cell walls contain a large amount of SiC. Figure 5 shows a μcell wall prior and after an in-situ tensile test. The fracture starts at the places indicated by the arrows. During the test the upper crack propagates to the top of the image and the lower crack to the bottom of the image, the crack is bridged by a small piece of material. Figure 6 is a close-up of the lower crack initiation point. The video as well as figure 6 clearly show that locally the crack initiates in a β -AlFeSi plate and that the crack propagates through the β -AlFeSi plate. As the crack reaches the end of a β -AlFeSi plate it continues in another plate located nearby. In this way it propagates through the network of randomly orientated and homogeneously distributed plates (see figure 5). About half of the fracture

surface of the cell wall of figure 5 is covered with the β -AlFeSi plates. The β -AlFeSi plates run through the large grains and across the grain boundaries from one grain into another. Therefore the fracture path is transgranular and the grains do not play a large role in the fracture behavior. Figure 6c depicts the fracture surfaces of figure 6b and clearly shows that the fracture of the precipitates is due to cleavage.

4. Discussion

It is clear that fracture initiates in and propagates through the β -AlFeSi plates, which decreases the ductility of cell walls and struts considerably and leads to brittle fracture of the entire foam. When the β -AlFeSi plates are removed the ductility is expected to increase. One way to decrease the amount of β -AlFeSi plates is by decreasing the concentration of Fe in the alloy, since the amount β -AlFeSi plates scales with the concentration of Fe and not of Si (i.e. due to the excess of Si). The exact origin of the high amount of Fe in the aluminum melt is unclear. It can be due to the variability of the precursor or due to contamination of the aluminum with Fe during the foaming or the recycling. Another way to decrease the amount of AlFeSi-plates is through the cooling rate (the size of the AlFeSi-precipitates decreases with increasing cooling rate⁸) although this is probably difficult to achieve in the manufacturing process of metal foams. An additional way to increase cell wall ductility would be to change the β -phase into the α -phase. When the phase of the precipitates changes from β -AlFeSi to α -AlFeSi, the coverage decreases due to the morphology of the α -phase. The formation of the α -phase can be promoted by a proper heat treatment of the foam or by adding certain transition elements to the alloy prior to the solidification⁵. Nevertheless, the exact influence of the α -phase (with or without a heat treatment) on the ductility of the cell wall is unknown. When β -AlFeSi plates are removed from the microstructure the strength and ductility of the cell walls depends on the size distribution, strength distribution and volume fraction of the SiC particles. According to reference 10 aluminum matrix composites with a high

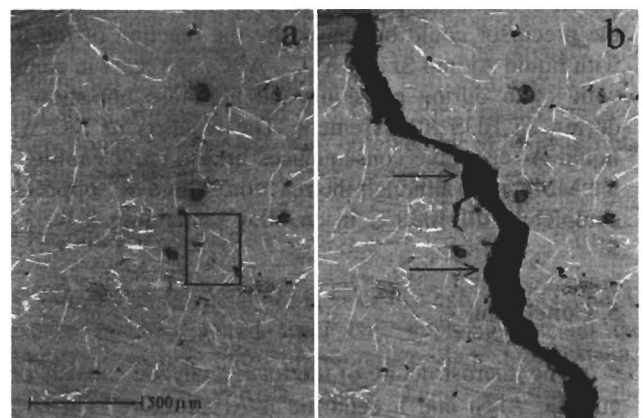


Fig. 5: (a) BSE image of the cell wall used in the in-situ tensile test prior to deformation. Black square indicates the area of figure 6. (b) Cell wall after deformation. Black arrows indicate initiation points.

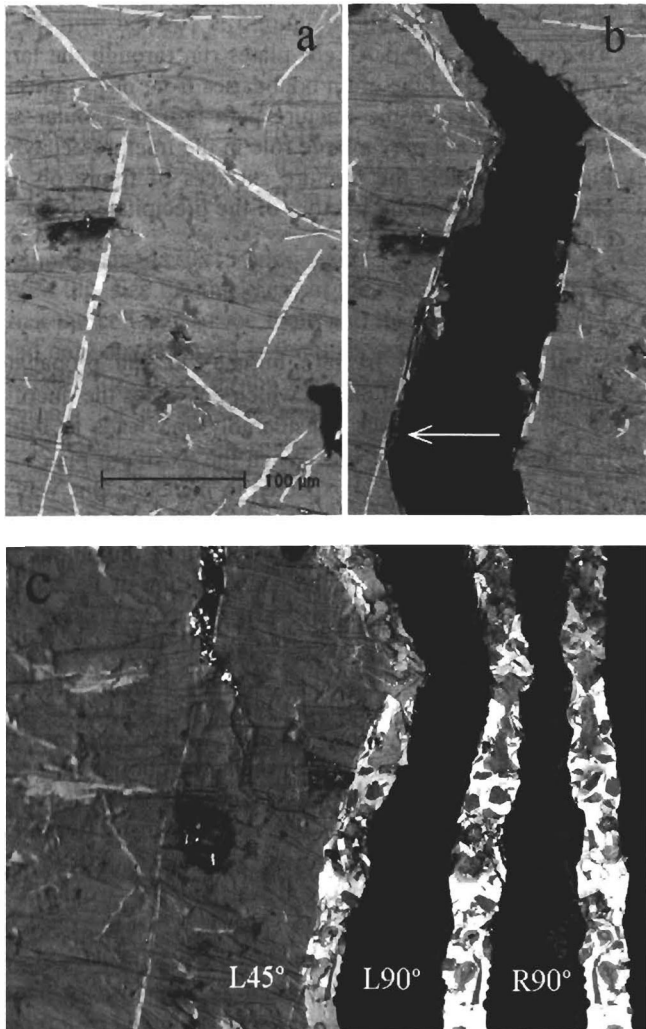


Fig. 6 (a) BSE image of the area marked by the black square in fig. 5a, prior to deformation. (b) After deformation, white arrow indicates the point of initiation. (c) Left fracture surface at 45° and 90° and the right fracture surface at 90°

volume fraction of ceramic particles can be **tough**, strong and relatively ductile, but it depends sensitively on the **strength** distribution of the particles. No special attention was paid to the SiC because the effect of the β -AlFeSi plates on the fracture behavior is larger. The increase of the Si concentration measured with EDS compared with the precursor could be caused by the reaction of the SiC with liquid Al into Si and Al_4C_3 . Al_4C_3 can react in contact with water **during** polishing and therefore not show up **during** an EDS measurement. The reaction of SiC with liquid Al can have consequences on the recyclability of the MMC melt although the reaction should be suppressed completely till 1050°C in an alloy containing 8 wt% of Si^[11].

5. Conclusion

The **microstructure** of the foam analyzed consists of a eutectic Al-Si and a dendritic α -Al structure. The **grain** size is about 500-1000 μm , which is much larger than the dendritic structure. SiC particles are on or just below the Al-gas interface. Fe, present in the melt, forms plates of β -AlFeSi during solidification of the aluminum foam, which

are 50-200 μm in length and homogeneously distributed. Fracture of a cell wall initiates in a β -AlFeSi plate, which **spans** the whole thickness of the usually 40 μm thick cell wall. The crack propagates through other β -AlFeSi plates, resulting in a brittle fracture of the cell wall due to the high amount of homogeneously distributed β -AlFeSi plates.

Evidently the high amount of β -AlFeSi plates has an detrimental effect on the fracture behavior of foam made **from** a **cast** aluminum alloy. The reason is that **during** solidification Fe has enough time to form large plates of β -AlFeSi that **span** the entire cell wall thickness. However, the cooling rate (being inversely proportional to the plate size) cannot easily be controlled **during** processing. Since Al and Si are abundantly present, the amount of β -AlFeSi plates scales with the concentration of Fe. For that reason the Fe concentration should be kept as low as possible **during** the (re)foaming. This should increase the distance between the β -AlFeSi plates which in **turn** slows the crack propagation and increases the cell wall ductility.

Acknowledgements

We would like to **thank** Dietmar Leitmeier for his support as well as the ESA International for the Trainee grant for N. Babcsán. Financial support **from** the Foundation for Fundamental Research on Matter (FOM-Utrecht) and the Netherlands Institute for Metals Research is **gratefully** acknowledged.

REFERENCES

- 1) D. Leitmeier, H-P. Degischer and H.J. Frankl: *Adv. Eng. Mat.* **4** (10) (2002) 735-740.
- 2) N. Babcsán, D. Leitmeier and J. Banhart: *Colloid. Surface. A* 261 (2005) 123-130.
- 3) C. San Marchi, J-F. Despois and A. Mortensen: *Acta Mater.* **52** (2004) 2895-2902.
- 4) E. Amsterdam, P.R. Onck and J.T.M. De Hosson: *J. Mat. Sci.* **40** (2005) 5813-5819.
- 5) M.H. Mulazimoglu, A. Zaluska, J.E. Grusleski and F. Paray: *Met. Trans.* **27A** (1996) 929-936.
- 6) F.H. Samuel, A.M. Samuel, H.W. Doty and S Valtierra: *Met. Trans.* **32A** (2001) 2061-2075.
- 7) W. Khalifa, F.H. Samuel and J.E. Grusleski: *Met. Trans* **34A** (2003) 807-825.
- 8) B. Dutta and M. Rettenmayr: *Mat. Sci. Eng. A* **283** (2000) 218-224.
- 9) M. Hansen: *Constitution of Binary Alloys*, Sec. Ed., (McGraw-Hill Book Company, New York, 1958) pp. 90-95.
- 10) A. Miserez, R. Müller, A. Rossoll, L. Weber and A. Mortensen: *Mat. Sci. Eng. A* **387-389** (2004) 822-831
- 11) T. Fan, D. Zhang, G. Yang, T. Shibayanagi, M. Naka, T. Sakata and H. Mori: *Composites: Part A* **34** (2003) 291-299.